A quantum mechanical study of dehydration vs. decarbonylation of formamide catalysed by amorphous silica surfaces

Quantum mechanical study of dehydration *vs* decarbonylation of formamide catalysed by amorphous silica surfaces

Stefano Pantaleone,[a,§,*] Clara Salvini,[b,c,§] Lorenzo Zamirri,[b] Matteo Signorile,[b] Francesca Bonino,[b] and Piero Ugliengo[b,*]

[a.] *Univ. Grenoble Alpes, CNRS, Institut de Planétologie et d'Astrophysique de Grenoble (IPAG), 38000 Grenoble, France.*
[b.] *Dipartimento di Chimica and Nanostructured Interfaces and Surfaces (NIS) Centre, Università degli Studi di Torino, via P. Giuria 7, IT-10125, Torino, Italy.*
[c.] *Now at: Dipartimento di Scienza Applicata e Tecnologia, Politecnico di Torino, Corso Duca degli Abruzzi 24, Torino 10129, Italy.*

§ Authors contributed equally to this work.

* Corresponding author: piero.ugliengo@unito.it, stefano.pantaleone@unito.it

Electronic Supplementary Information (ESI) available: structures and cartesian coordinates of all the optimized steps of the reactions considered in the present work (Figures S1-S10), energetic values of all the reactions considered in the present work, also including different starting points as reference state (Table S1-S4), basis sets. See DOI: 10.1039/x0xx00000x

Abstract

Formamide is abundant in the interstellar medium and was also present during the formation of the Solar system through the accretion process of the interstellar dust. Within the physico-chemical conditions of the primordial Earth it could have undergone decomposition, either via dehydration (HCN + H_2O) or decarbonylation (CO + NH_3). The first reactive channel provides HCN, which is an essential molecular building block for the formation of RNA/DNA bases, crucial for the emergence of life on Earth. In this work we studied, at CCSD(T)/pVTZ level, the two competitive routes of formamide decomposition, *i.e.* dehydration and decarbonylation, either in liquid formamide (by using the polarization continuum model technique), and at the interface between liquid formamide and amorphous silica. Amorphous silica was adopted as a convenient model of the crystalline silica phases, ubiquitous present in the primordial (and actual) Earth crust, and also due to its relevance in catalysis, adsorption and chromatography. Results show that: i) silica surface sites catalyse both decomposition channels by reducing the activation barriers of about 100 kJ mol^{-1} with respect to the reactions in homogeneous medium, and ii) the dehydration channel, giving rise to HCN, is strongly favoured from a kinetic standpoint over decarbonylation, the latter being, instead, slightly favoured from a thermodynamic point of view.

Introduction

The comprehension of how life originated on Earth is one of the most emerging and fascinating challenges of science, requiring a multidisciplinary approach owing to its intrinsic complexity. Indeed, in a recent influential publication entitled "Reinventing Chemistry",[1] G.M. Whitesides has gathered a list of new class of problems for the future chemistry and two of them dealt with prebiotic and planetary chemistry. Several theories have been proposed to explain the driving force that led to the cascade of events from which complex biological polymers, (such as DNA, RNA and proteins) took origin.[2–5] However, at the basis of these hypothesis, the starting point towards the formation of polymeric species from monomeric building blocks (nucleobases and amino acids), requires the presence of simple molecules like water (H_2O), carbon dioxide (CO_2) and monoxide (CO), ammonia (NH_3), and methane (CH_4). Such a scenario necessarily entails to find out possible chemical pathways towards life from both thermodynamic and kinetic points of view focusing on the research of potential molecules and the chemical and physical interactions implicated.[3,6]

Among the possible key molecules within the above context, formamide (NH_2CHO) is of special interest as:

- it is abundant in the interstellar medium, and consequently, on the Earth, according to several recent theories;[7–12]
- it is the smallest molecule envisaging the peptide bond while involving four out of six of the fundamental chemical elements essential for life (hydrogen, carbon, oxygen, nitrogen, phosphorus and sulphur);[13–18]
- it decomposes in simple molecules such as H_2O, CO, NH_3, and hydrogen cyanide (HCN). While water, carbon monoxide and ammonia are relatively stable molecules, HCN is particularly reactive as it polymerizes leading to the formation of the DNA/RNA nucleobases, in particular to adenine ($C_5N_5H_5$), an HCN pentamer.[13,19,20]

The gradual organization of simple molecules through building blocks up to biopolymers, is a complex process involving many chemical reactions, and, in turn, requiring sources of energy to occur. According to a seminal hypothesis by Bernal,[21] one of the crucial steps for the emergence of life on Earth could have taken place at the interface with mineral surfaces.[22–29] As a result of many experimental and computational studies, it has been demonstrated that mineral surfaces can interact with molecules increasing their concentration by adsorption processes as well as protect them from hostile environmental conditions and, finally, by acting as catalysts, to promote the reaction pathways to specific products .[3,30–39] Among the several minerals, crystalline silica phases (SiO_2) are of particular interest as catalyst for prebiotic reactions as they are among the most abundant species composing the Earth's surface (47,9%).[40,41] Moreover, previous studies show that the nature of silica surface (exposed faces, density of terminal hydroxyl groups, etc.) and its physicochemical properties make it able to interact with biomolecules and that the surface sites, namely the Si-OH terminations, are shared by both crystalline and amorphous silica surfaces.[42–44] In case of formamide, bare silica proves to be able to drive its reactivity and selectivity towards specific products (mostly purine and cytosine, which are the final product of

polymerization of many HCN molecules),[14,45] but it also catalyses the nucleophilic attack of an amine with a carboxylic group to form the amide bond.[34] Moreover, several experimental studies have highlighted the role of mineral surfaces (among which also silica) in the synthesis of nucleobases and related species from formamide.[14,16,18,26,45–48] The adoption of an amorphous silica model in the present work, rather than one derived from crystalline silica (more relevant in a prebiotic context) is to provide data for future experiments, which are usually carried out on amorphous silica owing to the much higher surface area compared with the crystal samples, facilitating the characterization of the adsorption process by spectroscopic and thermodynamic means.

Many theoretical studies have been carried out on the decomposition reactions of formamide. Wang et al. studied the decomposition process of formamide until the recombination of one the most important intermediates (HCN) to finally form purine and adenine molecules,[49,50] which is the most interesting chemical route from a prebiotic scenario viewpoint. However, many studies have also been carried out to study other competitive reaction channels, such as dehydrogenation ($HNCO + H_2$), decarbonylation ($NH_3 + CO$) besides the dehydration one ($HCN + H_2O$),[51,52] by means of MD simulations,[53] and also in the liquid phase (water solvent).[54] Other studies have taken into account the decomposition of formamide through free radical routes,[55] also considering formamide and protonated formamide in electron excited states (both singlet and triplet).[56] Similar processes, but occurring at the interface with mineral surfaces, have been studied by Nguyen et al. with very *naïve* TiO and VO molecular models mimicking the extended solids,[57] and by Masumi and co-workers at the interface with silicon-carbide nanotubes.[58] However, an accurate description of the reaction steps involving realistic models for silica surfaces and formamide towards the production of HCN is entirely missing in the literature.

In the present work, we performed a computational study aimed to predict the dehydration ($HCN + H_2O$) pathway of formamide in competition with the decarbonylation channel ($NH_3 + CO$) on selected amorphous silica surface models. These surfaces were simulated starting from periodic models we have already adopted in previous works carried out in our laboratory, and they have been tested to give good results in predicting silica surface properties.[59,60] Kinetically, both reactive channels involve rather complex activated processes: for the HCN formation (the most relevant one in the prebiotic context), the strong C=O double bond of formamide must break. Usually this is achieved by invoking a multi-step mechanism through the imine species via an intra-molecular proton transfer from the $–NH_2$ group to the C=O group. The imine is higher in energy than formamide as the resonance structures favour the latter over the former (see Scheme 1).

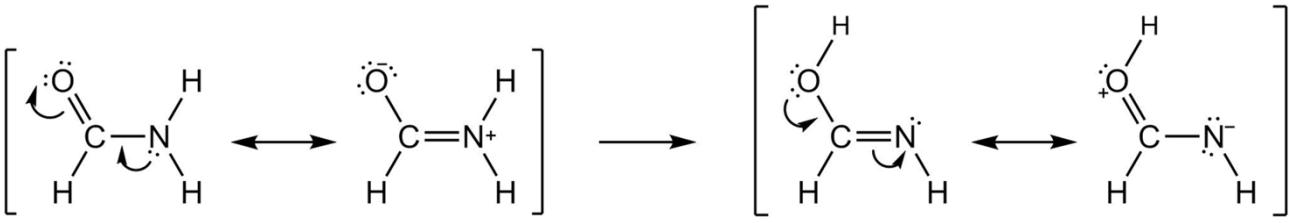

Scheme 1: Resonance forms of formamide (left) and of the corresponding imine (right).

In the paper, we will address the following processes, all envisaging results obtained through the PCM method in liquid formamide, *a prebiotic scenario where the first biological oligomers might be formed:*[61] i) the uncatalyzed formamide dehydration and decarbonylation, and ii) the same reactions catalysed by the two silica models, respectively with low (SiA, 1.5 SiOH nm^{-2}) and high (SiB, 4.5 SiOH nm^{-2}) degree of surface hydroxylation.

Methods

Computational Details. As the present work only involves molecular clusters, we used the Gaussian09 package for all calculations.[62] Geometry optimizations have been performed within the density functional theory (DFT) framework at PBE-D2 level,[63] where D2 is the Grimme's *a posteriori* correction for dispersive interactions.[64] We relied on the Ahlrichs' TZVP[65,66] basis set (BS) on all atoms as this is characterized by a reduced basis set superposition error (BSSE).[67,68] Further details of the adopted BS are reported in the Electronic Supplementery Information (ESI) file available online. In order to improve the energetic description, we refined the PBE-D2/TZVP potential energy surfaces (PESs) through single point (SP) energy corrections at CCSD(T)[69,70]/cc-pVTZ[71,72] level on the PBE-D2/TZVP optimised structures for reactions involving formamide alone, and up to two water molecules as catalysts. When silica models were considered, due to the increased size of the system compared with the previous cases, we adopted the ONIOM2 approach[73–76] in which the high-level (CCSD(T)/cc-pVTZ) zone involves the formamide molecule and all the interacting –OH moieties belonging to the silanol groups of the silica model, and the low level zone (PBE-D2/TZVP) all the remaining atoms. When referring to ONIOM2 results in the structures represented along this work, the high-level zone is in a ball and stick representation, while the low-level one is shown as sticks. To mimic the real system in which formamide reacts in its own liquid phase,[61] we run all the optimizations using the polarized continuum model (PCM)[77–81] with the dielectric constant of formamide (ε = 109.0). Results on gas-phase calculations are reported in the ESI for comparison. Frequency calculations have been performed on the PBE-D2/TZVP optimized geometries to check for minima (all real frequencies) or for first order saddles points (transition states – TSs – all but one real frequencies) of the PESs. Moreover, the thermodynamic quantities have been calculated at the temperature of 433 K, at which the decomposition of formamide and the synthesis of nucleic bases becomes appreciable.[13–16,18,25,46–48] The final energy profiles reported

along this work have been obtained in the following way: for each species (reactants, intermediates, TSs and products) we transformed CCSD(T)/cc-pVTZ and ONIOM2(CCSD(T)/cc-pVTZ:PBE-D2/TZVP) electronic energies into Gibbs free energies through the classical harmonic oscillator/rigid rotor approximations computed at the PBE-D2/TZVP level. Gaussian thermochemistry have been corrected through the quasi-harmonic approximation, proposed by Grimme,[82] in which frequencies lower than the 100 cm^{-1} cut-off are replaced by free rotor modes. This improves the calculation of the thermal corrections, which would be otherwise underestimated when considering very low frequency values. To avoid discontinuity close to the cut-off, a damping function was used to interpolate the values computed with the two approaches.

Kinetic rate constants k were computed through the Eyring equation:[83,84]

$$\boldsymbol{k = (k_B T/h) e^{\Delta G^{\ddagger}/RT}}$$

where k_B is the Boltzmann constant, T the absolute temperature, R the ideal gas constant, h the Plank constant and $\Delta G^{\ddagger}$ is the difference of free energy between the transition state and the previous corresponding minimum. The half-life times $t_{1/2}$ have been estimated assuming a first-order kinetic, as:

$$\boldsymbol{t_{1/2} = ln2/k}$$

The graphical visualization and structural manipulation of structures was performed with the MOLDRAW program.[85] Images were rendered with the POVRAY code.

When reactions occurred at the silica surfaces via an adsorption step from the liquid case (as in the modelled reactions), the choice of the energy reference is somehow ill-defined. One possibility is to consider the energy of the non-interacting reactants as a reference: in this case, the adsorption and reaction energies are assumed to be all canalized into the reactions serving to overcome specific kinetic barriers. The second most realistic possibility adopted in this work, is to consider the reactants (*i.e.* the initial intermolecular complexes) as the reference, assuming that the adsorption energy is dissipated through the lattice modes of the adsorbent (the amorphous silica). This choice is also more wisely balanced when considering the free energy. Indeed, if one considers the free reactants as reference, the entropic contribution is a function of the number of involved species (moving from one component for the free formamide reaction to two for SiA and SiB cases) which severely bias the final free energy profile. For all these reasons we decided to focus, in this work, on reaction profiles computed using, as reference, the formamide in its most stable interaction with silica.

Surface models. For the reasons explained before (*vide supra*), experimentally, the adsorption of formamide is usually carried out on the amorphous silica; therefore, as in a previous work of ours, we resorted to amorphous models derived from Ref. 54. In particular, to explore the energy path of the formamide decomposition on silica, we used a cluster model cut out from a periodic model envisaging about 1.5 silanol (Si–OH) groups nm^{-2} already adopted by Signorile et al.,[60] hereafter refereed as SiA (low OH density). We also studied the formamide decomposition at an amorphous silica model exhibiting about 4.5 silanol groups nm^{-2}, hereafter referred as SiB (high OH density). These two situations mimic the cases of an amorphous silica calcined at very high T (around 1000 K), while SiB is a silica outgassed at 298 K, in which adsorbed water molecules are removed from the surface.[34] The periodic models are shown in Figure 1. Atoms in blue, forming the outermost "crown" of the cluster models, are fixed to their periodic positions, in order to simulate the rigidity of the solid, while atoms in red, representing the innermost part of the cluster models inclusive of the hydroxyl groups, are free to move during the geometry optimization procedures. To preserve the correct valence of the atoms forming the external crown, the atoms cut out from the periodic models have been replaced with hydrogens. Specifically, we proceeded in the following way: once these H atoms have been included in the models, we optimized their positions at PBE-D2/TZVP level, fixing the positions of all the other atoms forming the cluster. Then, when the formamide decomposition has been investigated, the positions of the H atoms have been also kept fixed as well as all atoms in blue in Figure 1.

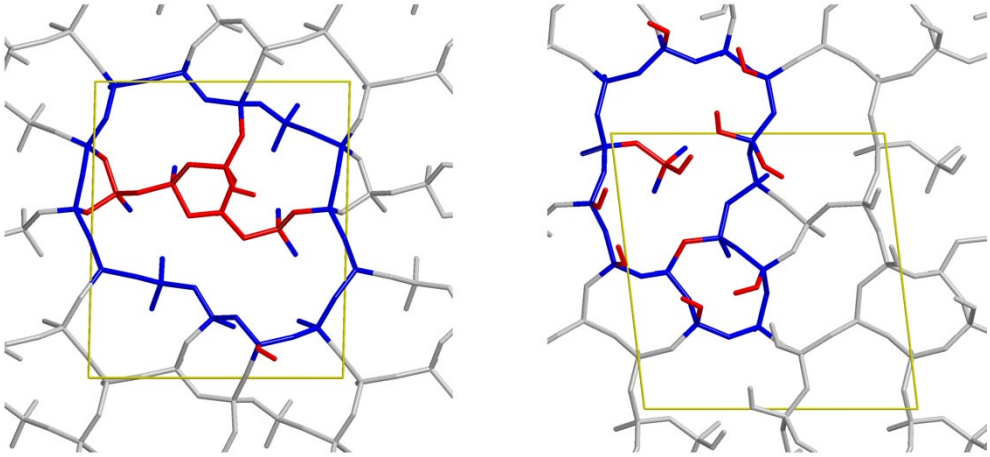

Figure 1: Cluster models (blue + red atoms) defined from the amorphous silica periodic slabs (in grey colour). Left: SiA model (about 1.5 silanol groups nm^{-2}); right: SiB model (about 4.5 silanol groups nm^{-2}). Blue: atoms frozen to the positions resulted in the periodic model. Red: atoms free to move during the geometry optimization. Unit cell borders in yellow colour.

Results

Non-catalysed formamide dehydration and decarbonylation.

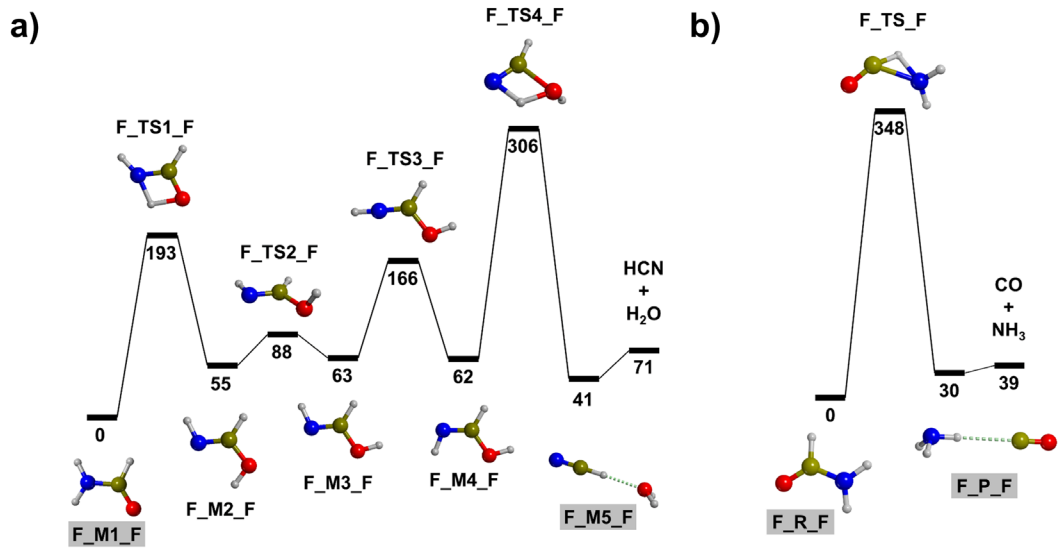

Figure 2: CCSD(T)/cc-pVTZ//PBE-D2/TZVP reaction profile (ΔG_{433}) for the formamide dehydration (section a) and decarbonylation (section b) in PCM (F). Gibbs free energies are in kJ mol^{-1}. Hydrogen in white, oxygen in red, carbon in ochre, nitrogen in blue.

The formamide intramolecular dehydration path (Figure 2a) exhibits very high energy barriers due to the strained four-member ring in two different transition states (F_TS1_F and F_TS4_F in Figure 2a). Another problematic step is the CIS/TRANS conversion of the imine group. Because of its nature, free rotation around the C=N double bond is hindered, and the CIS/TRANS conversion occurs through the C-N-H bending (forming a quasi linear C-N-H angle in the corresponding TS, F_TS3_F). The second reaction step involves a conformational change (free rotation along a dihedral angle), and, accordingly, has a lower energy barrier (F_TS2_F) compared with the other ones.

The formamide intramolecular decarbonylation path (Figure 2b) is a single-step reaction, which involves a proton transfer from the carbon to the nitrogen atoms and, in a concerted fashion, the C—N bond cleavage. It also has a very high activation barrier, even higher than that of the dehydration process, as, in this case, the mechanism envisages a proton transfer with a highly strained three-member ring and the pseudo-double peptide bond cleavage.

From a thermodynamic point of view, the decarbonylation is favoured compared with dehydration, in particular if we consider the non-interacting products as reference state. The difference between interacting and free products of the two reactive channels, 20 kJ mol^{-1} and 9 kJ mol^{-1} for the dehydration and decarbonylation, respectively, is due to the different H-bonds strength, which are stronger for the HCN···H_2O system and, accordingly, more difficult to be broken.

Formamide dehydration at the amorphous silica surfaces. As described before, we adopted two different silica models with a different superficial concentration of silanol (Si–OH) groups to represent high (SiB, 4.5 Si–OH nm^{-2}) and low (SiA, 1.5 Si–OH nm^{-2}) hydroxylated surfaces, respectively.

In line with the non-assisted reaction (Figures 2a), the most critical steps are: i) the two proton transfers, SiA_TS1_F and SiA_TS5_F (in particular the second one, involving the cleavage of the C–O bond); ii) the CIS/TRANS conversion of imine (SiA_TS4_F). The SiA-catalysed formamide dehydration (Figure 3) shows a consistent lowering of the reaction barriers involving the proton transfer (of about 90-100 kJ mol^{-1}) with respect to the non-catalysed reaction, thanks to the amphoteric behaviour of the silanol group acting as proton shuttle, a behaviour which has been already shown to be efficient in a recent paper by Rimola et al.[86] This is a direct consequence of the formation of a less strained, six-member ring in the SiA_TS1_F and SiA_TS5_F structures. In the silica catalysed case the reaction presents one more step involving the rotation of the dihedral angle of the silanol group (SiA_TS3_F).

Figure 4 shows the reaction pathway of formamide dehydration catalysed by the hydrophilic silica model, SiB. Here, the higher concentration of silanol groups (4.5 Si–OH nm^{-2}) with respect to the hydrophobic SiA one (1.5 Si–OH nm^{-2}) leads to the presence of neighbouring silanol groups, which, in principle, should help the proton transfer by a further expansion of the transition state ring from six (SiA_TS1_F and SiA_TS5_F of Figure 4) to eight (SiB_TS1_F and SiB_TS5_F of Figure 5) members.

Despite that, the comparison of the two pathways, SiA_TS5_F and SiB_TS5_F shows the same barriers (153 kJ mol^{-1} with respect to the previous intermediate), while the first step is even more hindered on the hydrophobic silica (67 kJ mol^{-1}) than on the hydrophilic model (75 kJ mol^{-1}). As for the thermodynamics of the reaction, the global free reaction energy variations are 107 and 147 kJ mol^{-1} for the hydrophobic and for the hydrophilic silica catalysed reactions, respectively. *We want to caution the reader: the differences in thermodynamic values depend on the choice of the starting minimum. We just want to point out that these values, despite different from those in the gas phase, still are endoergonic, and, accordingly the choice of the starting minimum is physically reasonable.*

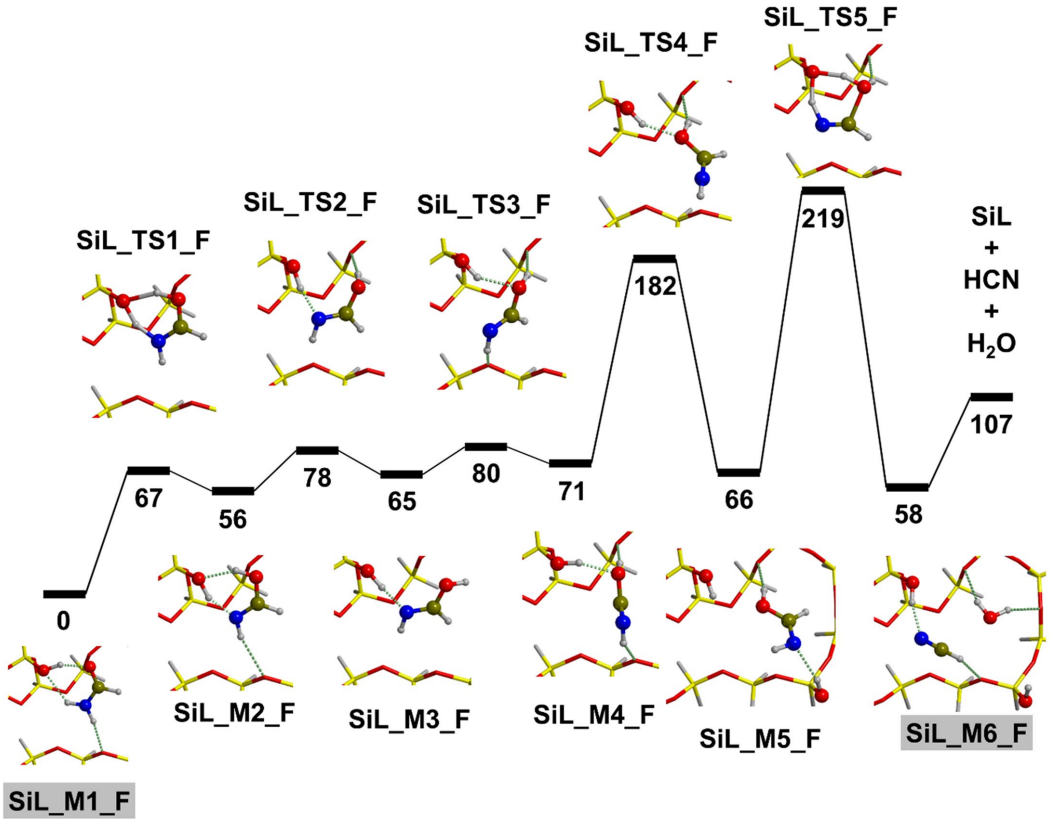

Figure 3: ONIOM[CCSD(T)/cc-pVTZ:PBE-D2/TZVP)//PBE-D2/TZVP] reaction profile (ΔG_{433}) for the formamide dehydration catalysed by the hydrophobic SiA silica model. Free energies in kJ mol^{-1}. Hydrogen in white, oxygen in red, carbon in ochre, nitrogen in blue, silicon in yellow.

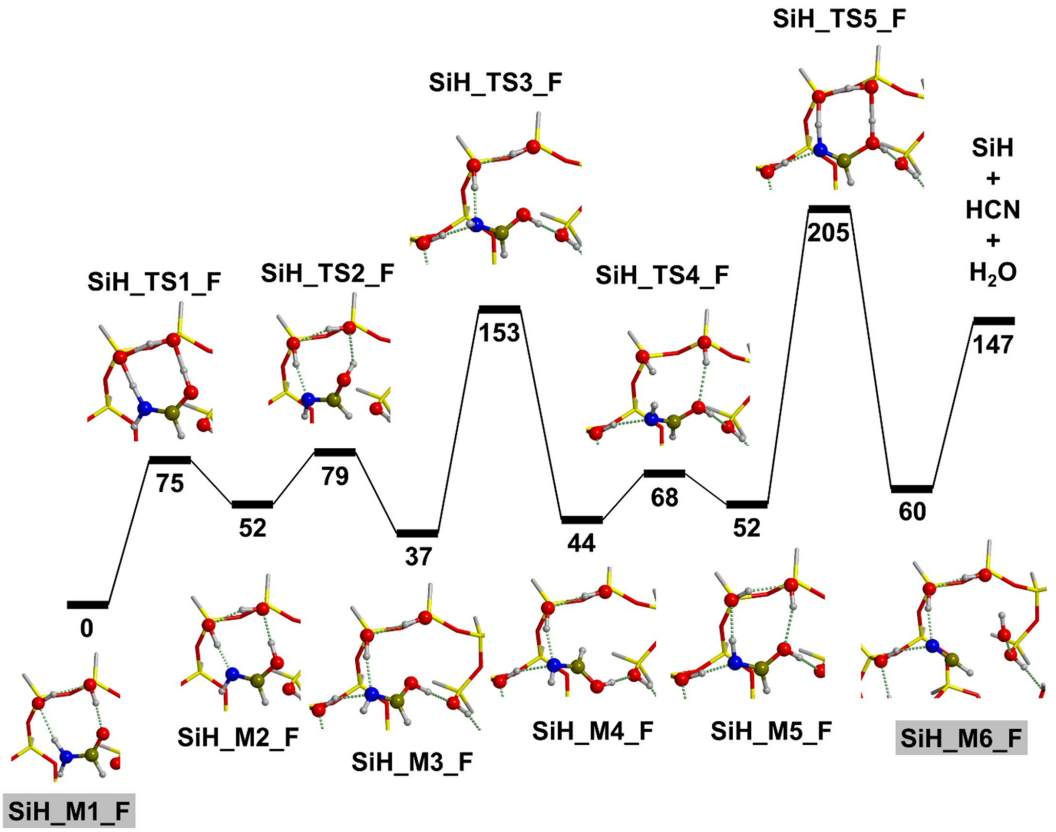

Figure 4: ONIOM[CCSD(T)/cc-pVTZ:PBE-D2/TZVP)//PBE-D2/TZVP] reaction profile (ΔG_{433}) for the formamide dehydration catalysed by the hydrophilic SiB silica model. Free energies in kJ mol^{-1}. Hydrogen in white, oxygen in red, carbon in ochre, nitrogen in blue, silicon in yellow.

Formamide decarbonylation at the amorphous silica surfaces.

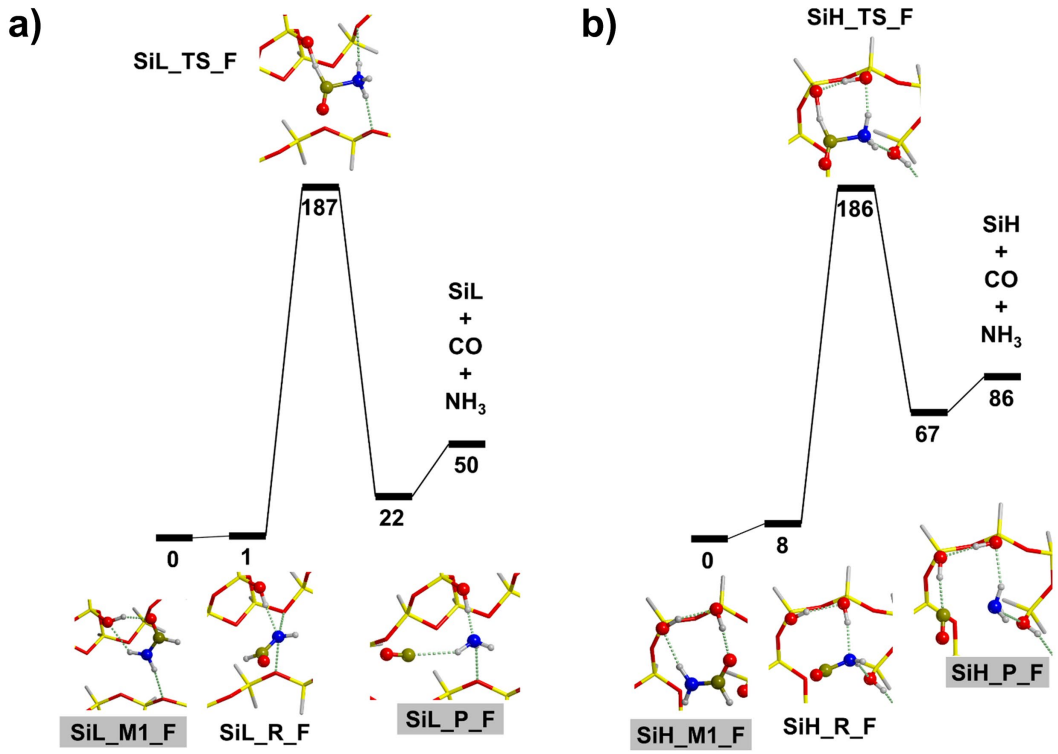

Figure 5: ONIOM[CCSD(T)/cc-pVTZ:PBE-D2/TZVP)//PBE-D2/TZVP] reaction profile (ΔG_{433}) for the formamide decarbonylation catalysed by: a) the hydrophobic SiA silica model; b) the hydrophilic SiB silica model. Free energies in kJ mol^{-1}. Hydrogen in white, oxygen in in red, carbon in ochre, nitrogen in blue, silicon in yellow.

Figure 5a shows the formamide decarbonylation pathway catalysed by hydrophobic silica. As for the non-catalysed reaction (Figure 2b) it follows a concerted mechanism. Also, in this case, the surface silanol groups assist the proton transfer, dropping the barrier down by a large amount with respect to the gas phase reaction (from 347 to 187 kJ mol^{-1}).

The thermodynamics of the process seems to be competitive with the non-catalysed reaction: regarding the interacting products, the process is more favourable in the presence of the silica surface (8 kJ mol^{-1} of difference), while considering the non-interacting ones the non-catalysed reaction is favoured (11 kJ mol^{-1} of difference).

As observed for the dehydration reactive channel, the silanol groups cooperation at hydrophilic SiB silica (Figure 5b) does not provide a remarkable effect on the activation barrier (178 kJ mol^{-1}), which is only 8 kJ mol^{-1} lower than the reaction on the hydrophobic silica.

Comparison between the two amorphous silica models. From a kinetic viewpoint, both SiA/SiB silica models (hydrophobic and hydrophilic) have a high impact in stabilizing the transition states, through the expansion of the critical small intramolecular rings involving proton transfers by the proton shuttle operated by the surface silanol groups. However, the comparison between the two silica cases reveals that the high cooperativity of silanol groups on the hydrophilic SiB model does not exert a significant role compared with the hydrophobic SiA model, where this effect is missing. As regards the two different reactive channels, the formamide dehydration catalysed reactions occur in few tens of hours. The decarbonylation channel, despite the slightly higher barriers, presents very long half-life times due to the exponential relationship relating free energy with the kinetic constant.

As regards the thermodynamics, in both the reactive channels the non-interacting products are more favourable on hydrophobic silica than on the hydrophilic one. On the hydrophilic silica, the higher silanol content involves a higher number of H-bond interactions with the reaction products. These H-bonds on the hydrophilic silica are strengthened by the cooperative effects between silanol groups. These combining effects hinder the release of the products from the silica surface to the liquid phase. For all considered cases, the reactions are endoergonic, therefore relatively high temperatures are needed for the reaction to occur. Accordingly, the thermodynamic corrections have been computed at 433 K together with the rate constants and half-life times (see Table 1).

Table 1: Activation energies (E_a), rate constants (k), and half-life times ($t_{1/2}$) for all the reactions considered in the present work. NC stands for the non-catalysed reaction. Energies in kJ mol^{-1}. Rate constants in $seconds^{-1}$. Half-life times in hours.

	NC	SiA	SiB
E_a^{dehydr}	244.3	153.1	152.4
E_a^{decarb}	348.3	185.7	178.2
k^{dehydr}	3.04E-17	3.06E-06	3.68E-06
k^{decarb}	8.67E-30	3.62E-10	2.87E-09
$t_{1/2}^{dehydr}$	6.33E+12	6.30E+01	5.24E+01
$t_{1/2}^{decarb}$	2.22E+25	5.32E+05	6.70E+04

Conclusions

In the present work the formamide decomposition has been studied by means of accurate quantum simulations considering two different reactive channels: the dehydration (HCN + H_2O) and the decarbonylation (NH_3 + CO). These reactions have been simulated either in the homogeneous liquid formamide phase (by using the polarization continuum model method) and at the interface between liquid formamide phase and two different cluster models (SiA, hydrophobic and SiB hydrophilic) of amorphous silica, a common and widespread material, whose surface functionalities are shared also by crystalline silica (α-quartz), present in the prebiotic era. The aim is to evaluate the silica catalytic effect on the formamide decomposition with respect to the intramolecular decomposition in liquid phase. *This is important to understand how the first biological macromolecules (like DNA/RNA) have been produced by the polymerization of building blocks (nitrogenous bases) which, in turn, are synthesized by even smaller monomers (adenine ($C_5H_5N_5$) from HCN).*[19,20]

We can summarize the most important results as follows:

- silanol SiOH groups at the silica surface are key sites to assist the formamide decomposition, facilitating the proton transfer from one formamide moiety to the other. The calculated half-life times decrease dramatically due to the silica interaction compared with the non-catalysed reactions;
- the efficiency of the two silica models as catalysts is very similar, despite the higher density of silanol groups on the hydrophilic model;
- as regards the two reactive channels, the kinetics of the decarbonylation is much slower than the dehydration process despite being more favourable from a thermodynamic point of view. This is an important result, because the dehydration leads to the production of HCN, which is a molecule of great interest from a prebiotic standpoint, as its polymerization represents a key brick for the formation of DNA/RNA nitrogenous bases.

Conflicts of interest

There are no conflicts to declare.

Acknowledgements

MS, FB and PU acknowledge financial supported from the Italian MIUR and from Scuola Normale Superiore (project PRIN 2015, STARS in the CAOS - Simulation Tools for Astrochemical Reactivity and Spectroscopy in the Cyberinfrastructure for Astrochemical Organic Species, cod. 2015F59J3R). SP acknowledges funding from European Union's Horizon 2020 research and innovation program, the European Research Council (ERC) Project “the Dawn of Organic Chemistry”, grant agreement No 741002.

References

1. G. M. Whitesides, Reinventing chemistry, *Angew. Chem. Int. Ed.*, 2015, **54**, 3196–3209.
2. F. Hoyle and C. Wickramasinghe, *Lifecloud. The origin of life in the universe*, J. M. Dent and Sons, London, 1978.
3. N. Kitadai and S. Maruyama, Origins of building blocks of life: A review, *Geosci. Front.*, 2018, **9**, 1117–1153.
4. E. D. Andrulis, Theory of the Origin, Evolution, and Nature of Life, *Life*, 2012, **2**, 1–105.
5. A. Pross and R. Pascal, The origin of life: what we know, what we can know and what we will never know, *Open. Biol.*, 2013, **3**, 120190.
6. K. Ruiz-Mirazo, C. Briones and D. Escosura, Prebiotic Systems Chemistry: New Perspectives for the Origins of Life, *Chem. Rev.*, 2014, **114**, 285–366.
7. L. Song and J. Kästner, Formation of the prebiotic molecule NH_2CHO on astronomical amorphous solid water surfaces: accurate

tunneling rate calculations, *Phys. Chem. Chem. Phys.*, 2016, **18**, 29278–29285.
8. A. Lòpez-Sepulcre, A. A. Jaber, E. Mendoza, B. Lefloch, C. Ceccarelli, C. Vastel, R. Bachiller, J. Cernicharo, C. Codella, C. Kahane, M. Kama and M. Tafalla, Shedding light on the formation of the pre-biotic molecule formamide with ASAI, *Mon. Not. R. Astron. Soc.*, 2015, **449**, 2438–2458.
9. V. Barone, C. Latouche, D. Skouteris, F. Vazart, N. Balucani, C. Ceccarelli and B. Lefloch, Gas-phase formation of the prebiotic molecule formamide: insights from new quantum computations, *Mon. Not. R. Astron. Soc.*, 2015, **435**, L31–L35.
10. C. Kahane, C. Ceccarelli, A. Faure and E. Caux, Detection of Formamide, the Simplest but Crucial Amide, in a Solar-Type Protostar, *Astrophys. J. Lett.*, 2013, **763**, L38.
11. A. Rimola, D. Skouteris, N. Balucani, C. Ceccarelli, J. Enrique-Romero, V. Taquet and P. Ugliengo, Can Formamide Be Formed on Interstellar Ice? An Atomistic Perspective, *ACS Earth Sp. Chem.*, 2018, **2**, 720–734.
12. J. Enrique-Romero, A. Rimola, C. Ceccarelli, P. Ugliengo, N. Balucani and D. Skouteris, Reactivity of HCO with CH_3 and NH_2 on Water Ice Surfaces. A Comprehensive Accurate Quantum Chemistry Study, *ACS Earth Sp. Chem.*, 2019, **3**, 2158–2170.
13. R. Saladino, C. Crestini, F. Ciciriello, G. Costanzo and E. Di Mauro, Formamide Chemistry and the Origin of Informational Polymers, *Chem. Biodivers.*, 2007, **4**, 694–720.
14. R. Saladino, C. Crestini, G. Costanzo, R. Negri and E. Di Mauro, A Possible Prebiotic Synthesis of Purine, Adenine, Cytosine, and 4(3H)-Pyrimidinone from Formamide: Implications for the Origin of Life, *Bioorgan. Med. Chem.*, 2001, **9**, 1249–1253.
15. G. Costanzo, R. Saladino, C. Crestini, F. Ciciriello and E. Di Mauro, Formamide as the main building block in the origin of nucleic acids, *Evol. Bio.*, 2007, **7**, S1.
16. R. Saladino, C. Crestini, V. Neri, F. Ciciriello, G. Costanzo and E. Di Mauro, Origin of Informational Polymers: The Concurrent Roles of Formamide and Phosphates, *ChemBioChem*, 2006, **7**, 1707–1714.
17. M. Ferus, D. Nesvorný, J. Šponer, P. Kubelík, R. Michalčíková, V. Shestivská, J. E. Šponer and S. Civiš, High-energy chemistry of formamide: A unified mechanism of nucleobase formation, *Proc. Natl. Acad. Sci. USA*, 2015, **112**, 657–662.
18. R. Saladino, C. Crestini and E. Di Mauro, Advances in the Prebiotic Synthesis of Nucleic Acids Bases: Implications for the Origin of Life, *Curr. Org. Chem.*, 2004, **8**, 1425–1443.
19. J. Orò, Synthesis of Adenine from Ammonium Cyanide, *Biochem. Bioph. Res. Co.*, 1960, **2**, 407–412.
20. J. Orò, Mechanism of Synthesis of Adenine from Hydrogen Cyanide under Possible Primitive Earth Conditions, *Nature*, 1961, **4794**, 1193–1194.
21. J. D. Bernal, The Physical Basis of Life, *Proc. Phys. Soc. B*, 1949, **62**, 597–618.
22. R. M. Hazen, Mineral surfaces and the prebiotic selection and organization of biomolecules, *Am. Miner.*, 2006, **91**, 1715–1729.
23. R. M. Hazen, D. Papineau, W. Bleeker, R. T. Downs, J. M. Ferry, T. J. McCoy, D. A. Sverjensky and H. Yang, Mineral evolution, *Am. Miner.*, 2008, **93**, 1693–1720.
24. R. M. Hazen and D. A. Sverjensky, Mineral Surfaces, Geochemical Complexities, and the Origins of Life, *Cold Spring Harb. Perspect. Biol.*, 2010, **2**, a002162.
25. R. Saladino, G. Botta, M. Delfino and E. Di Mauro, Meteorites as Catalysts for Prebiotic Chemistry, *Chem. Eur. J.*, 2013, **19**, 16916–16922.
26. L. Rotelli, J. M. Trigo-Rodríguez, C. E. Moyano-Cambero, E. Carota, L. Botta, E. Di Mauro and R. Saladino, The key role of meteorites in the formation of relevant prebiotic molecules in a formamide/water environment, *Sci. Rep.*, 2016, **6**, 38888.
27. S. D. Senanayake and H. Idriss, Photocatalysis and the origin of life: Synthesis of nucleoside bases from formamide on TiO_2 (001) single surfaces, *Proc. Natl. Acad. Sci. USA*, 2006, **103**, 1194–1198.
28. J. M. R. Muir and H. Idriss, Surface Science Formamide reactions on rutile TiO_2 (011) surface, *Surf. Sci.*, 2009, **603**, 2986–2990.
29. A. Rimola, M. Sodupe and P. Ugliengo, Role of mineral surfaces in prebiotic chemical evolution. In silico quantum mechanical studies, *Life*.
30. S. Pantaleone, A. Rimola and M. Sodupe, Canonical, Deprotonated, or Zwitterionic? A Computational Study on Amino Acid Interaction with the TiO_2 (101) Anatase Surface, *J. Phys. Chem. C*, 2017, **121**, 14156–14165.
31. W. H. Yu, N. Li, D. S. Tong, C. H. Zhou, C. Z. Lin and C. Y. Xu, Adsorption of proteins and nucleic acids on clay minerals and their interactions: A review, *Appl. Clay Sci.*, 2013, **80–81**, 443–452.
32. S. Pantaleone, P. Ugliengo, M. Sodupe and A. Rimola, When the Surface Matters: Prebiotic Peptide-Bond Formation on the TiO_2 (101) Anatase Surface through Periodic DFT-D2 Simulations, *Chem. Eur. J.*, 2018, **24**, 16292–16301.
33. A. Rimola, M. Sodupe and P. Ugliengo, Aluminosilicate Surfaces as Promoters for Peptide Bond Formation: An Assessment of Bernal's Hypothesis by ab Initio Methods, *J. Am. Chem. Soc.*, 2007, **129**, 8333–8344.
34. A. Rimola, M. Fabbiani, M. Sodupe, P. Ugliengo and G. Martra, How Does Silica Catalyze the Amide Bond Formation under Dry Conditions? Role of Specific Surface Silanol Pairs, *ACS Catal.*, 2018, **8**, 4558–4568.
35. G. Martra, C. Deiana, Y. Sakhno, I. Barberis, M. Fabbiani, M. Pazzi and M. Vincenti, The Formation and Self-Assembly of Long Prebiotic Oligomers Produced by the Condensation of Unactivated Amino Acids on Oxide Surfaces, *Angew. Chem. Int. Ed.*, 2014, **53**, 4671–4674.
36. H. Hashizume, Adsorption of Nucleic Acid Bases, Ribose, and Phosphate by Some Clay Minerals, *Life*, 2015, **5**, 637–650.
37. E. Biondi, S. Branciamore, M. Maurel and E. Gallori, Montmorillonite protection of an UV-irradiated hairpin ribozyme: evolution of the RNA world in a mineral environment, *Evol. Bio.*, 2007, **7**, S2.
38. F. Scappini, F. Casadei, R. Zamboni, M. Franchi, E. Gallori and S. Monti, Protective effect of clay minerals on adsorbed nucleic acid against UV radiation: possible role in the origin of life, *Int. J. Astrobiol.*, 2004, **3**, 17–19.
39. P. Mignon, P. Ugliengo and M. Sodupe, Theoretical Study of the Adsorption of RNA/NA Bases on the External Surfaces of Na^+-Montmorillonite, *J. Phys. Chem. C*, 2009, **113**, 13741–13749.
40. J. W. Morgan and E. Anderst, Chemical composition of Earth, Venus, and Mercury, *Proc. Natl. Acad. Sci. USA*, 1980, **77**, 6973–6977.
41. W. F. Mcdonougha and S. -s. Sun, The composition of the Earth, *Chem. Geol.*, 1995, **120**, 223–253.

42. A. Rimola, S. Tosoni, M. Sodupe and P. Ugliengo, Does Silica Surface Catalyse Peptide Bond Formation? New Insights from First-Principles Calculations, *ChemPhysChem*, 2006, **7**, 157–163.
43. A. Rimola, P. Ugliengo and M. Sodupe, Formation versus Hydrolysis of the Peptide Bond from a Quantum-mechanical Viewpoint: The Role of Mineral Surfaces and Implications for the Origin of Life, *Int. J. Mol. Sci.*, 2009, **10**, 746–760.
44. A. Rimola, D. Costa, M. Sodupe, J.-F. Lambert and P. Ugliengo, Silica Surface Features and Their Role in the Adsorption of Biomolecules: Computational Modeling and Experiments, *Chem. Rev.*, 2013, **113**, 4216–4313.
45. G. Botta, B. M. Bizzarri, E. Di Mauro and J. M. G. Ruiz, A Global Scale Scenario for Prebiotic Chemistry: Silica-Based Self- Assembled Mineral Structures and Formamide, *Biochemistry*, 2016, **55**, 2806–2811.
46. R. Saladino, U. Ciambecchini, C. Crestini, G. Costanzo, R. Negri and E. Di Mauro, One-Pot TiO_2-Catalyzed Synthesis of Nucleic Bases and Acyclonucleosides from Formamide: Implications for the Origin of Life, *ChemBioChem*, 2003, **4**, 514–521.
47. R. Saladino, C. Crestini, U. Ciambecchini, F. Ciciriello, G. Costanzo and E. Di Mauro, Synthesis and Degradation of Nucleobases and Nucleic Acids by Formamide in the Presence of Montmorillonites, *ChemBioChem*, 2004, **5**, 1558–1566.
48. R. Saladino, C. Crestini, V. Neri, J. R. Brucato, L. Colangeli, F. Ciciriello, E. Di Mauro and G. Costanzo, Synthesis and Degradation of Nucleic Acid Components by Formamide and Cosmic Dust Analogues, *ChemBioChem*, 2005, **6**, 1368–1374.
49. J. Wang, J. Gu, M. T. Nguyen, G. Springsteen and J. Leszczynski, From Formamide to Purine: A Self-Catalyzed Reaction Pathway Provides a Feasible Mechanism for the Entire Process, *J. Phys. Chem. B*, 2013, **117**, 9333–9342.
50. J. Wang, J. Gu, M. T. Nguyen, G. Springsteen and J. Leszczynski, From Formamide to Adenine: A Self-Catalytic Mechanism for an Abiotic Approach, *J. Phys. Chem. B*, 2013, **117**, 14039–14045.
51. V. S. Nguyen, T. M. Orlando, J. Leszczynski and M. T. Nguyen, Theoretical Study of the Decomposition of Formamide in the Presence of Water Molecules, *J. Phys. Chem. A*, 2013, **117**, 2543–2555.
52. V. S. Nguyen, H. L. Abbott, M. M. Dawley, T. M. Orlando, J. Leszczynski and M. T. Nguyen, Theoretical Study of Formamide Decomposition Pathways, *J. Phys. Chem. A*, 2011, **115**, 841–851.
53. A. Gahlaut and M. Paranjothy, Unimolecular decomposition of formamide via direct chemical dynamics simulations, *Phys. Chem. Chem. Phys.*, 2018, **20**, 8498–8505.
54. F. Pietrucci and A. M. Saitta, Formamide reaction network in gas phase and solution via a unified theoretical approach: Toward a reconciliation of different prebiotic scenarios, *Proc. Natl. Acad. Sci. USA*, 2015, **112**, 15030–15035.
55. Y. A. Jeilani, H. T. Nguyen, D. Newallo, J.-M. D. Dimandja and M. T. Nguyen, Free radical routes for prebiotic formation of DNA nucleobases from formamide, *Phys. Chem. Chem. Phys.*, 2013, **15**, 21084–21093.
56. H. T. Nguyen, V. S. Nguyen, N. T. Trung, R. W. A. Havenith and M. T. Nguyen, Decomposition Pathways of the Neutral and Protonated Formamide in Some Lower-Lying Excited States, *J. Phys. Chem. A*, 2013, **117**, 7904–7917.
57. H. T. Nguyen and M. T. Nguyen, Decomposition pathways of formamide in the presence of vanadium and titanium monoxides, *Phys. Chem. Chem. Phys.*, 2015, **17**, 16927–16936.
58. M. D. Esrafili, R. Nurazar and V. Masumi, Surface Science Adsorption and decomposition of formamide over zigzag (n,0) silicon-carbide nanotubes (n = 5–7): Investigation of curvature effects, *Surf. Sci.*, 2015, **637**–**638**, 69–76.
59. P. Ugliengo, M. Sodupe, F. Musso, I. J. Bush, R. Orlando and R. Dovesi, Realistic Models of Hydroxylated Amorphous Silica Surfaces and MCM-41 Mesoporous Material Simulated by Large-scale Periodic B3LYP Calculations, *Adv. Mater.*, 2008, **20**, 4579–4583.
60. M. Signorile, C. Salvini, L. Zamirri, F. Bonino, G. Martra, M. Sodupe and P. Ugliengo, Formamide Adsorption at the Amorphous Silica Surface: A Combined Experimental and Computational Approach, *Life*, 2018, **8**, 42.
61. J. L. Bada, J. H. Chalmers and H. J. Cleaves, Is formamide a geochemically plausible prebiotic solvent?, *Phys. Chem. Chem. Phys.*, 2016, **18**, 20085–20090.
62. Gaussian 09, Revision D.01, M. J. Frisch, G. W. Trucks, H. B. Schlegel, G. E. Scuseria, M. A. Robb, J. R. Cheeseman, G. Scalmani, V. Barone, G. A. Petersson, H. Nakatsuji, X. Li, M. Caricato, A. V. Marenich, J. Bloino, B. G. Janesko, R. Gomperts, B. Mennucci, H. P. Hratchian, J. V. Ortiz, A. F. Izmaylov, J. L. Sonnenberg, Williams, F. Ding, F. Lipparini, F. Egidi, J. Goings, B. Peng, A. Petrone, T. Henderson, D. Ranasinghe, V. G. Zakrzewski, J. Gao, N. Rega, G. Zheng, W. Liang, M. Hada, M. Ehara, K. Toyota, R. Fukuda, J. Hasegawa, M. Ishida, T. Nakajima, Y. Honda, O. Kitao, H. Nakai, T. Vreven, K. Throssell, J. A. Montgomery Jr., J. E. Peralta, F. Ogliaro, M. J. Bearpark, J. J. Heyd, E. N. Brothers, K. N. Kudin, V. N. Staroverov, T. A. Keith, R. Kobayashi, J. Normand, K. Raghavachari, A. P. Rendell, J. C. Burant, S. S. Iyengar, J. Tomasi, M. Cossi, J. M. Millam, M. Klene, C. Adamo, R. Cammi, J. W. Ochterski, R. L. Martin, K. Morokuma, O. Farkas, J. B. Foresman and D. J. Fox, Gaussian, Inc., Wallingford CT, 2009.
63. J. P. Perdew, K. Burke and M. Ernzerhof, Generalized Gradient Approximation Made Simple, *Phys. Rev. Lett.*, 1996, **77**, 3865–3868.
64. S. Grimme, Semiempirical GGA-Type Density Functional Constructed with a Long-Range Dispersion Correction, *J. Comput. Chem.*, 2006, **27**, 1787–1799.
65. A. Schäfer, H. Horn and R. Ahlrichs, Fully optimized contracted Gaussian basis sets for atoms Li to Kr, *J. Chem. Phys.*, 1992, **97**, 2571–2577.
66. A. Schäfer, C. Huber and R. Ahlrichs, Fully optimized contracted Gaussian basis sets of triple zeta valence quality for atoms Li to Kr, *J. Chem. Phys.*, 1994, **100**, 5829–5835.
67. H. B. Jansen and P. Ros, Non-Empirical Molecular Orbital Calculations on the Protonation of Carbon Monoxide, *Chem. Phys. Lett.*, 1969, **3**, 140–143.
68. B. Liu and A. D. McLean, Accurate calculation of the attractive interaction of two ground state helium atoms., *J. Chem. Phys.*, 1973, **59**, 4557–4558.
69. J. A. Pople, M. Headgordon and K. Raghavachari, Quadratic configuration interaction. A general technique for determining electron correlation energies, *J. Chem. Phys.*, 1987, **87**, 5968–5975.
70. G. D. Purvis and R. J. Bartlett, A full coupledcluster singles and doubles model: The inclusion of disconnected triples, *J. Chem. Phys.*, 1982, **76**, 1910–1918.

71. T. H. Dunning, Gaussian basis sets for use in correlated molecular calculations. I. The atoms boron through neon and hydrogen, *J. Chem. Phys.*, 1989, **90**, 1007–1023.
72. R. A. Kendall and T. H. Dunning, Electron affinities of the first-row atoms revisited. Systematic basis sets and wave functions, *J. Chem. Phys.*, 1992, **96**, 6796–6806.
73. F. Maseras and K. Morokuma, IMOMM: A New Integrated Ab Initio + Molecular Mechanics Geometry Optimization Scheme of Equilibrium Structures and Transition States, *J. Comput. Chem.*, 1995, **16**, 1170–1179.
74. T. Vreven and K. Morokuma, On the Application of the IMOMO (Integrated Molecular Orbital + Molecular Orbital) Method, *J. Comput. Chem.*, 2000, **21**, 1419–1432.
75. T. Vreven, K. Suzie Byun, I. Komàromi, S. Dapprich, J. A. Montgomery Jr., K. Morokuma and M. J. Frisch, Combining Quantum Mechanics Methods with Molecular Mechanics Methods in ONIOM, *J. Chem. Theory Comput.*, 2006, **2**, 815–826.
76. S. Dapprich, I. Komáromi, K. S. Byun, K. Morokuma and M. J. Frisch, A new ONIOM implementation in Gaussian98. Part I. The calculation of energies, gradients, vibrational frequencies and electric field derivatives, *J. Mol. Struct.-Theochem*, 1999, **461–462**, 1–21.
77. M. Cossi, V. Barone, R. Cammi and J. Tomasi, Ab initio study of solvated molecules: a new implementation of the polarizable continuum model, *Chem. Phys. Lett.*, 1996, **255**, 327–335.
78. B. Mennucci and J. Tomasi, Continuum solvation models: A new approach to the problem of solute' s charge distribution and cavity boundaries, *J. Chem. Phys.*, 1997, **106**, 5151–5158.
79. E. Cancès, B. Mennucci and J. Tomasi, A new integral equation formalism for the polarizable continuum model: Theoretical background and applications to isotropic and anisotropic dielectrics, *J. Chem. Phys.*, 1997, **107**, 3032–3041.
80. V. Barone, M. Cossi and J. Tomasi, A new definition of cavities for the computation of solvation free energies by the polarizable continuum model, *J. Chem. Phys.*, 1997, **107**, 3210–3221.
81. V. Barone, M. Cossi and J. Tomasi, Geometry Optimization of Molecular Structures in Solution by the Polarizable Continuum Model, *J. Comput. Chem.*, 1998, **19**, 404–417.
82. S. Grimme, Supramolecular binding thermodynamics by dispersion-corrected density functional theory, *Chem. Eur. J.*, 2012, **18**, 9955–9964.
83. M. G. Evans and M. Polanyi, Some applications of the transition state method to the calculation of reaction velocities, especially in solution, *Trans. Faraday Soc.*, 1935, **31**, 875–894.
84. H. Eyring, The Activated Complex in Chemical Reactions, *J. Chem. Phys.*, 1935, **3**, 107–115.
85. P. Ugliengo, D. Viterbo and G. Chiari, MOLDRAW: Molecular graphics on a personal computer, *Zeitschrift fur Krist. - New Cryst. Struct.*, 1993, **207**, 9–23.
86. A. Rimola, M. Sodupe and P. Ugliengo, Amide and Peptide Bond Formation: Interplay between Strained Ring Defects and Silanol Groups at Amorphous Silica Surfaces, *J. Phys. Chem. C*, 2016, **120**, 24817–24826.